

## First-principles study of hydrogen permeation in palladium-gold alloys

Shucheng Xu, Parveen Sood, M. L. Liu, and Angelo Bongiorno

Citation: *Appl. Phys. Lett.* **99**, 181901 (2011); doi: 10.1063/1.3656739

View online: <http://dx.doi.org/10.1063/1.3656739>

View Table of Contents: <http://apl.aip.org/resource/1/APPLAB/v99/i18>

Published by the [American Institute of Physics](#).

---

### Additional information on *Appl. Phys. Lett.*

Journal Homepage: <http://apl.aip.org/>

Journal Information: [http://apl.aip.org/about/about\\_the\\_journal](http://apl.aip.org/about/about_the_journal)

Top downloads: [http://apl.aip.org/features/most\\_downloaded](http://apl.aip.org/features/most_downloaded)

Information for Authors: <http://apl.aip.org/authors>

## ADVERTISEMENT



**AIP** | Applied Physics Letters

Accepting Submissions in  
Biophysics and Bio-Inspired Systems

*Submit Today*

**AIP**  
Publishing

## First-principles study of hydrogen permeation in palladium-gold alloys

Shucheng Xu,<sup>1,2</sup> Parveen Sood,<sup>1</sup> M. L. Liu,<sup>2</sup> and Angelo Bongiorno<sup>1,a)</sup>

<sup>1</sup>*School of Chemistry and Biochemistry, Georgia Institute of Technology, Atlanta, Georgia 30332-0400, USA*

<sup>2</sup>*School of Material Science and Engineering, Georgia Institute of Technology, Atlanta, Georgia 30332-0245, USA*

(Received 11 August 2011; accepted 9 October 2011; published online 31 October 2011)

Density functional theory and lattice model calculations are combined to study the permeability of hydrogen in Pd lightly alloyed with Au. This study shows that small amounts of Au substitutions in Pd leads to, respectively, an increase and decrease of the diffusivity and solubility of hydrogen in the alloy. The competition between these two phenomena depends on temperature and can yield dilute PdAu membranes with a hydrogen permeability higher than pure Pd. © 2011 American Institute of Physics. [doi:10.1063/1.3656739]

Palladium-based membranes are used industrially to separate H<sub>2</sub> from a hydrocarbon feedstock.<sup>1,2</sup> To prevent embrittlement of the membrane and increase its resistance to poisoning by gas contaminants, Pd is alloyed with metals such as Au, Ag, and Cu.<sup>3,4</sup> Alloying inevitably influences other key parameters such as the permeability of H. Unexpectedly, however, at low alloying levels Pd membranes show values of the H permeability higher than in pure Pd.<sup>5-9</sup> The origin of this behavior is still elusive to date. This first-principles study addresses this issue in the case of PdAu alloys.

Experimental reports on the enhanced permeability of H in PdAu alloys date back to 1869.<sup>5</sup> Today, this issue is still matter of both experimental<sup>7-9</sup> and theoretical<sup>10-13</sup> scrutiny. Experiments show that at very low Au contents the permeability of the alloy is larger than that of Pd.<sup>6,9</sup> A maximum permeability, about 1.3 times larger than in pure Pd, has been reported to be attained between 4 and 6 wt. % Au.<sup>6-9</sup> At higher Au contents, the permeability of H drops rapidly, due to both a reduced solubility and diffusivity.<sup>6-9</sup> The origin of these behaviors has been attributed to microstructure and defects of the alloy<sup>6</sup> and to anomalous trends of either the diffusivity or solubility of H.<sup>6,9</sup> In the dilute regime, where the role of microstructure and defects can be disregarded, very recent experiments have shown that the higher value of permeability stems mainly from the larger diffusivity of H in the PdAu alloy.<sup>9</sup> This result, however, is in contrast with both earlier experiments, showing an almost constant diffusivity of H in dilute PdAu alloys,<sup>6,14</sup> and recent computational studies,<sup>12,13</sup> supporting the hypothesis that the permeability, follows the trend of the solubility.<sup>6</sup> This work addresses this issue. In particular, our results support the recent experimental findings of a H permeability dominated at low Au contents by a higher diffusivity.<sup>9</sup>

Spin polarized density functional theory (DFT) calculations were performed with the Vienna *ab initio* simulation package (VASP).<sup>15,16</sup> An energy cutoff of 400 eV was used for the planewaves, the exchange and correlation energy was computed as in Ref. 17, and ionic cores were treated by using the projector augmented wave method.<sup>18</sup>  $\Gamma$ -point cal-

culations were carried out by using cubic supercells including 108 metal atoms on a face-centered cubic (fcc) lattice. We considered the following metallic systems: perfect Pd and Au, and selected diluted PdAu alloys. The energy of H in a metal,  $\Delta E_H$ , was calculated by referring the total energy of the defected metal to those of the perfect metal and half H<sub>2</sub>. In our calculations, H was kept fixed in a selected interstitial position of the fcc lattice (Fig. 1), and the positions of the metal ions were optimized subjected to the constraint that their center of mass did not move. To assess the accuracy of our computational approach, a selected set of calculations were repeated by employing either a more recent exchange-correlation functional<sup>19</sup> or a  $2 \times 2 \times 2$  Monkhorst-Pack sampling grid of the Brillouin zone. These calculations showed that  $\Delta E_H$  are converged and that different approximations of the exchange-correlation energy introduce systematic errors of about 0.1-0.2 eV in  $\Delta E_H$ , while leaving almost unchanged ( $\leq 0.05$  eV) the relative energy values of H in different fcc interstitial positions.

H is soluble in Pd (Table I).  $\Delta E_H$  is negative within the interstices of the fcc lattice and, as expected, the lowest energy configuration of H in Pd is in correspondence of the octahedral ( $O_h$ ) site (Fig. 1). In a tetrahedral ( $T_d$ ) interstice, the energy of H raises by 0.04 eV. The so-called middle (M) and bridge (TS) interstitial sites (Fig. 1) correspond to metastable positions. Our calculations show that the lowest energy diffusion pathways of H in Pd consist of a sequence of  $O_h$ - $T_d$  steps, passing by M points. These diffusion steps involve energy barriers of 0.17 eV and 0.13 eV from the  $O_h$  to M site and from the M to  $T_d$  site, respectively (Fig. 1, top panel). TS sites are higher in energy than M points by about 0.4 eV. The transfer of H between two adjacent  $O_h$  or  $T_d$  sites via a TS point can thus be considered statistically irrelevant.

H is not soluble in Au. The computed values of  $\Delta E_H$  are found to be positive, both within the octahedral and tetrahedral interstices and along the high-symmetry segments joining the  $O_h$  and  $T_d$  sites (Fig. 1(b)). At variance with Pd,  $O_h$  sites in Au correspond to both high energy and metastable states of H. Stable configurations are found in correspondence of the  $T_d$  sites. These results show that Au substitutions in Pd modify non-trivially the energy landscape of H in PdAu alloys. Here, we focus on the low Au-content regime.

<sup>a)</sup>Electronic mail: angelo.bongiorno@chemistry.gatech.edu.

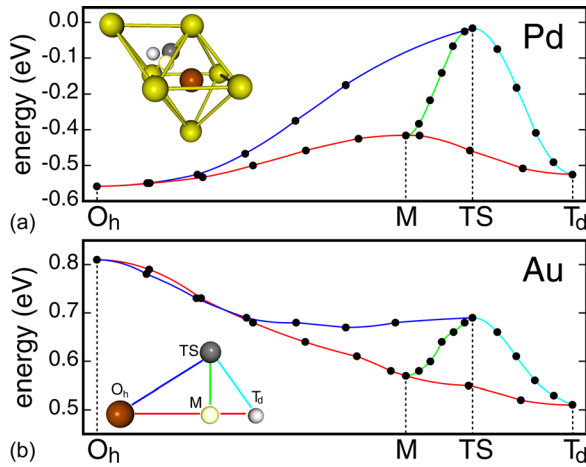


FIG. 1. (Color online) Energy of H in Pd (a) and Au (b) along high-symmetry directions of the fcc lattice (inset, (b)). Discs indicate DFT results while colored lines are guides to the eye. The inset in the top panel shows the location of the  $O_h$  (red),  $T_d$  (white), M (light yellow), and TS (gray) interstitial sites in a fcc lattice (yellow).

To model dilute PdAu alloys, we considered a 108-atom cubic supercell of fcc Pd with only one Au substitution, corresponding to a molar fraction of  $x \approx 0.01$ . Our calculations show that an isolated Au substitution in Pd changes the energy landscape of H only locally. The first next nearest neighbor  $O_h$  and  $T_d$  sites of Au remain stable positions for H, with energies higher than in pure Pd by 0.13 and 0.21 eV, respectively (Table I). The first next nearest neighbor M and TS sites of Au preserve a metastable character and raise in energy by more than 0.2 eV with respect to the same points in pure Pd (Table I). Beyond the first shell of nearest neighbor interstitial sites, the energy of H in the dilute alloy recovers the value as in pure Pd (Table I).

The energy profile of a H atom visiting  $O_h$  and  $T_d$  sites in contact with an isolated Au substitution in Pd is shown in Fig. 2. As in pure Pd, the  $O_h$  sites can be reached by crossing an energy barrier of 0.17 eV through a triangular constriction formed by Pd atoms only. To escape the  $O_h$  site, H can either cross an equivalent constriction with an activation energy of only 0.04 eV into a neighboring  $T_d$  cage or reach a  $T_d$  site in contact with the Au atom by crossing an energy barrier of 0.29 eV (Fig. 2). While the latter migration pathway is unfavorable, the former one occurs as likely as in pure Pd and, due to the nearly flat energy landscape inside the  $O_h$  interstice in contact with Au, it proceeds more readily. Overall, these results show that in dilute PdAu alloys the perme-

TABLE I.  $\Delta E_H$  (in eV) of H at high-symmetry interstitial sites in Pd, Au, and selected model PdAu alloys. Model Pd<sub>108-n</sub> Au<sub>n</sub> alloys are indicated with Au<sub>n</sub>,  $n = 1 \dots 6$ . Au<sub>1</sub> and Au<sub>1</sub><sup>Pd</sup> report the energy of H at sites belonging to the first and second shell of next nearest neighbor interstitial sites of the Au substitution, respectively. In Au<sub>n</sub>,  $n = 2 \dots 6$ , H is positioned in a  $T_d$  or  $O_h$  site and Au substitutions decorate the corresponding interstitial.

	Pd	Au	Au <sub>1</sub> <sup>Pd</sup>	Au <sub>1</sub>	Au <sub>2</sub>	Au <sub>3</sub>	Au <sub>4</sub>	Au <sub>5</sub>	Au <sub>6</sub>
$O_h$	-0.55	0.81	-0.56	-0.43	-0.17	-0.09	0.21	0.24	0.64
$T_d$	-0.51	0.51	-0.53	-0.32	-0.04	0.20	0.42	-	-
M	-0.38	0.58	-0.39	-0.14	-	-	-	-	-
TS	-0.02	0.69	-0.04	0.29	-	-	-	-	-

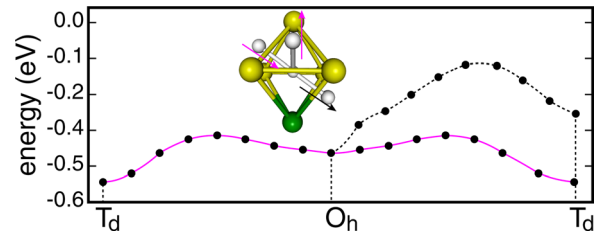


FIG. 2. (Color online) Energy profiles of a H atom diffusing across  $O_h$  and  $T_d$  cages near an isolated Au substitution in Pd. Symbols (DFT results) connected by the colored line show  $\Delta E_H$  along a  $T_d$ - $O_h$ - $T_d$  diffusion step in which only the  $O_h$  site lies within the first shell of next nearest neighbor interstitial sites of Au. Symbols connected by the black line show  $\Delta E_H$  of a H visiting  $O_h$ ,  $T_d$ , and M sites, all in the first shell of next nearest neighbor interstitial sites of Au. The diffusion steps (white ball and sticks, and arrows) are sketched in the inset (Au and Pd are shown in green and yellow, respectively).

ability of H varies with Au content because (1) the occupancy of the interstitial sites in direct contact with Au atoms decreases and (2) the migration process across the  $O_h$  interstices in contact with the Au substitutions occurs more favorably than in pure Pd.

To address the role of Au coordination, we considered a 108-Pd atom supercell and we inserted H in a  $O_h$  and  $T_d$  interstitial enclosed by an increasing number of Au substitutions, up to 6 and 4, respectively. Our DFT calculations show that  $\Delta E_H$  raises rapidly with the Au coordination (Table I). In particular, in an interstice fully surrounded by Au atoms, but otherwise embedded in pure Pd, H attains an energy very close to that as in pure Au. This result shows that first nearest-neighbor effects account for  $\sim 90\%$  of the differences of the energy of H in Pd and Au.

To study the permeability of H in dilute PdAu alloys, we used a simplified computational scheme. To represent the energy landscape of H in the alloy, we employed a periodic 3-D lattice model consisting of the  $O_h$ ,  $T_d$ , and M sites of a fcc lattice. TS sites were not included in the model, due to the high energy H attains at these positions. For a selected composition of the alloy, Au atoms were distributed at random in the fcc lattice, and, on the basis of the Au coordination, our results in Table I were used to assign energy values to the  $O_h$  and  $T_d$  sites. M points were assigned energy values of either  $-0.39$  eV or  $-0.14$  eV, depending whether or not a Au atom was in first shell of nearest neighbor metal ions. In the limit of low Au content, this lattice model is expected to represent well the geometrical and energetical features of the interstitial network visited by H during its diffusion.<sup>20,21</sup>

To estimate relative values of the H solubility, we used

$$\exp\left(-\frac{\mu_H^{\text{alloy}} - \mu_H^{\text{Pd}}}{k_B T}\right) = \frac{\mathcal{Z}^{\text{alloy}}}{\mathcal{Z}^{\text{Pd}}} \approx \frac{\sum_i e^{-\epsilon_i^{\text{alloy}}/k_B T}}{\sum_i e^{-\epsilon_i^{\text{Pd}}/k_B T}}, \quad (1)$$

where  $\mu_H$  and  $\mathcal{Z}$  are the chemical potential and partition function of H in the metallic systems and  $\epsilon_i$  are the site energies of the lattice model representation of the interstitial network in the metals. In the right side of Eq. (1), entropy and volume changes of  $\mu_H^{\text{alloy}}$  induced by Au substitutions are considered negligible.<sup>22</sup>

We used Eq. (1) to calculate the change relative to pure Pd of the solubility of H in Au<sub>x</sub> Pd<sub>1-x</sub> alloys with  $x \leq 0.12$

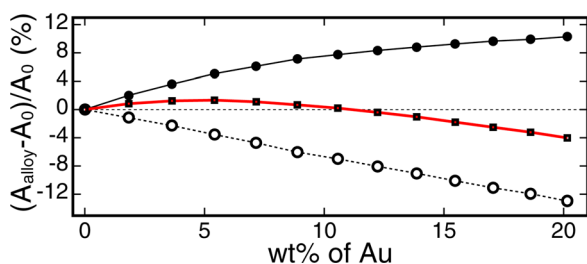


FIG. 3. (Color online) Relative percent values of the diffusion (discs), solubility (circles), and permeability (squares) coefficients of H in PdAu alloys vs. Au content, as obtained from lattice model and Monte-Carlo calculations. The coefficients for the alloy,  $A_{\text{alloy}}$ , are referred to those obtained for a pure and perfect Pd crystal,  $A_0$ . Diffusion and solubility values are calculated independently; their product gives the permeability coefficient. Lines are guides to the eye.

(20 wt% Au). In parallel, we used Monte Carlo simulations to calculate the change relative to pure Pd of the diffusion coefficient of H in the same alloys. Monte-Carlo steps consisted of either  $O_h-T_d$  or  $T_d-O_h$  elementary moves, and statistical occurrence was calculated according to transition state theory by accounting for the overall energy cost of the migration step, that is, crossing the M point and reaching a new solubility site. The diffusion coefficient was calculated via the Einstein relation. Values of permeability were obtained as product of the solubility and diffusion coefficients (Fig. 3).

Lattice model calculations at 300 K show that the diffusivity of H in dilute PdAu alloys is larger than in pure Pd (Fig. 3). The  $O_h$  solubility sites in close proximity of isolated Au substitutions raise in energy, creating spatial regions of nearly constant energy that can be accessed and rapidly crossed as frequently as in Pd (Fig. 2). According to our calculations, the competition between the decreasing solubility and increasing diffusivity leads to a maximum in the perme-

ability at about 5 wt% Au ( $x=0.03$ ), where it attains a value 1.33 times larger than that in pure Pd. At higher Au content, changes in the solubility dominate, causing the permeability to drop. This behavior of the permeability of H in PdAu alloys depends on temperature. At 400 K, for instance, Monte-Carlo calculations show that solubility dominates over diffusivity at all compositions, leading to a monotonically decreasing permeability. These results are in agreement with recent experiments on the diffusivity and permeability of H in dilute PdAu alloys.<sup>9</sup>

<sup>1</sup>E. Kikuchi, *Catal. Today* **25**, 333 (1985).

<sup>2</sup>M. Gryaznov, *Sep. Purif. Methods* **29**, 171 (2000).

<sup>3</sup>P. Kamakoti, B. D. Morreale, M. V. Ciocco, B. H. Howard, R. P. Killmeyer, A. V. Cugini, and D. S. Sholl, *Science* **307**, 569 (2005).

<sup>4</sup>O. Iyoha, R. Enick, R. Killmeyer, B. Howard, M. Ciocco, and B. Morreale, *J. Membr. Sci.* **306**, 103 (2007).

<sup>5</sup>T. Graham, *Proc. R. Soc. London* **17**, 212 (1869).

<sup>6</sup>Y. Sakamoto, S. Hirata, and H. Nishikawa, *J. Less-Common Met.* **88**, 387 (1985).

<sup>7</sup>S. K. Gade, E. A. Payzant, H. J. Park, P. M. Thoen, and J. D. Way, *J. Membr. Sci.* **340**, 227 (2009).

<sup>8</sup>K. E. Coulter, J. D. Way, S. K. Gade, S. Chaudhari, D. S. Sholl, and L. Semidey-Flecha, *J. Phys. Chem. C* **114**, 17173 (2010).

<sup>9</sup>T. B. Flanagan and D. Wang, *J. Phys. Chem. C* **115**, 11618 (2011).

<sup>10</sup>X. Ke and G. J. Kramer, *Phys. Rev. B* **66**, 184304 (2002).

<sup>11</sup>P. Kamakoti and D. S. Sholl, *Phys. Rev. B* **71**, 014301 (2005).

<sup>12</sup>C. G. Sonwane, J. Wilcox, and Y. H. Ma, *J. Phys. Chem. B* **110**, 24549 (2006).

<sup>13</sup>C. G. Sonwane, J. Wilcox, and Y. H. Ma, *J. Chem. Phys.* **125**, 184714 (2006).

<sup>14</sup>S. Maestas and T. J. Flanagan, *J. Phys. Chem.* **77**, 850 (1973).

<sup>15</sup>G. Kresse and J. Furthmüller, *Comput. Mater. Sci.* **6**, 15 (1996).

<sup>16</sup>G. Kresse and D. Joubert, *Phys. Rev. B* **59**, 1758 (1999).

<sup>17</sup>J. P. Perdew and Y. Wang, *Phys. Rev. B* **46**, 12947 (1992).

<sup>18</sup>P. E. Blöchl, *Phys. Rev. B* **50**, 17953 (1994).

<sup>19</sup>J. P. Perdew, K. Burke, and M. Ernzerhof, *Phys. Rev. Lett.* **77**, 3865 (1996).

<sup>20</sup>A. Bongiorno and A. Pasquarello, *Phys. Rev. Lett.* **88**, 125901 (2002).

<sup>21</sup>A. Bongiorno and A. Pasquarello, *Phys. Rev. B* **70**, 195312 (2004).

<sup>22</sup>S. Luo, D. Wang, and T. B. Flanagan, *J. Phys. Chem. B* **114**, 6117 (2010).